Impact of a dark boson mediated feeble interaction between dark matter and hadronic matter on the f-mode oscillation of neutron stars

Debashree Sen[1,*] and Atanu Guha[2,†]

[1]*Center for Extreme Nuclear Matters (CENuM), Korea University, Seoul 02841, Korea*
[2]*Department of Physics, Chungnam National University, 99, Daehak-ro, Yuseong-gu, Daejeon-34134, South Korea*

(Received 21 June 2024; accepted 1 October 2024; published 12 November 2024)

We studied the possible presence of dark matter (DM) in neutron stars (NSs) and the structural properties of the DM admixed NSs (DMANSs) in one of our recent works [1]. The feeble interaction between the fermionic DM (χ) with the hadronic matter is introduced through a dark scalar (ϕ) and a dark vector (ξ) boson as mediators. The allowed range of the mass of the fermionic DM (m_χ), for a particular range of DM Fermi momentum (k_F^χ), was obtained in the same work [1] with respect to the various astrophysical constraints on the structural properties of compact stars viz., the mass, radius, and tidal deformability. The present work is dedicated to the calculation and study of nonradial oscillation of the DMANSs using Cowling approximation. We particularly investigate the effect of the presence of DM on the fundamental (f) mode oscillation frequencies of the DMANSs utilizing the previously obtained range of m_χ for four different hadronic models. In this work we thoroughly investigate how the individual and combined effects of m_χ and k_F^χ affect the f-mode oscillation frequency. Within the framework of our DMANS models, for a particular value of k_F^χ, the range of $f_{\rm max}^{\rm DMANS}$, with respect to the allowed range of m_χ, is also obtained in the present work for four different hadronic models. Since in the present era, the 1.4 and $2.01 M_\odot$ NSs are of special interest after the detection of GW170817 and PSR J0740 + 6620, we particularly investigate, for the four hadronic models, the range of $f_{1.4}^{\rm DMANS}$ and $f_{2.01}^{\rm DMANS}$ with respect to the acceptable range of m_χ corresponding to the range of k_F^χ.

DOI: 10.1103/PhysRevD.110.103013

I. INTRODUCTION

Of the total energy budget of the Universe, the lion's share is made up of dark energy (about 70%), while the succeeding leading component is dark matter (around 25%). The so-called luminous matter, or the baryonic matter, makes up only 5% of the total energy content. At present, this is an unambiguously evident fact supported by certain astrophysical and cosmological observations [2–5]. To date several dedicated search methods have been implemented to obtain an idea about the interaction strength between the dark matter (DM) and standard model particles. The popular experimental search avenues, that include the direct and the indirect detection strategies [6,7], have shown significant developments. The most stringent constraints obtained to date are from the leading direct detection experiments like SuperCDMS [8], XENONnT [9], PandaX-II [10], DarkSide-50 [11], SENSEI [12], and LUX-ZEPLIN [13]. Experiments dedicated to indirect search are FERMI-LAT [14], IceCube [15], PAMELA [16,17], AMS-02 [18], Voyager [19], and CALET [20,21].

Significant advancement in the phenomenological aspects has also been made parallel to the progress of the experimental probes. One of the well-motivated methods to understand the properties of the DM particles and its interaction with baryonic matter is to explore the possible presence of DM in neutron stars (NSs) because NSs are highly gravitating objects that are capable of accreting matter from its surroundings including DM. Inside the NS core, matter is preserved at extreme conditions of density, pressure, compactness, and gravity. Fortunately, they are accessible by direct observations. Therefore, NSs serve the purpose of being unique natural astrophysical laboratories where we can investigate theoretically the properties of matter under extreme conditions. Several mechanisms can be responsible for the possible presence of DM in NSs, e.g., the capture or accretion of DM halo particles by NSs [22–26], the creation of its own DM through dark

*Contact author: debashreesen88@gmail.com
†Contact author: atanu@cnu.ac.kr

Published by the American Physical Society under the terms of the Creative Commons Attribution 4.0 International license. Further distribution of this work must maintain attribution to the author(s) and the published article's title, journal citation, and DOI. Funded by SCOAP³.

decays of neutrons [27–30], or inheritance of DM from the supernovae [31], etc. The DM particles end up being gravitationally bound to the star, and the DM particles attain thermal equilibrium among themselves due to the self-interactions [24,32]. This amply justifies the consideration of the DM particle density ρ_χ to be almost constant throughout the radius of the star [33–35]. The DM particles thus become structural parts of the NSs. This allows us to explore the effect of the presence of DM on the structural properties of NSs [1,34–39].

Within NS cores, DM may not interact with hadronic matter and the two types of matter coexist in the two fluid forms [37,40–54], whereas the interaction between the DM and the baryonic matter is also suggested by [31,33,39,55–59], mostly via the Higgs boson as mediator. In case the DM interacts with hadronic matter, the interaction must be extremely weak [60] to prevent the collapse of the star into a black hole. Therefore, we invoked feeble interaction between hadronic and fermionic DM χ via a new scalar mediator ϕ in [35] and also a dark vector mediator ξ in [1,34] in order to explain the possible existence of forming DM admixed NSs (DMANSs). ϕ and ξ interact with the hadronic matter ψ with a very feeble coupling strength. The masses of DM fermion (m_χ) and the mediators (m_ϕ and m_ξ) and their couplings (y_ϕ and y_ξ) are consistent with the self-interaction constraint from the Bullet cluster observations and from the present day relic abundance of DM, respectively. We concluded that the mass of DM plays a very important role in determining the structural properties of DMANSs. More massive the DM, the lesser are the maximum mass, radius and tidal deformability of the DMANSs. In [1] within a certain range of the constant DM particle density ρ_χ, we determined a possible range of m_χ for which the DMANSs satisfy the constraints on the structural properties of compact stars obtained from PSR J0740 + 6620 [61–63], gravitational wave (GW170817) data [64], and the NICER data for PSR J0030 + 0451 [65,66]. For this purpose, we considered certain relativistic mean field (RMF) models to account for the hadronic matter.

In [1] the suitable range of m_χ, consistent with the astrophysical constraints, was determined by calculating the structural properties like the mass, radius, and tidal deformability of the DMANSs. In the present work we focus on the phenomenon of nonradial NS oscillation and particularly on the fundamental or f-mode frequency of the oscillation of the DMANSs. One of the important reasons why the nonradial pulsations of NSs are of current interest is because they are connected with gravitational radiation. The oscillation of NSs is accompanied by the emission of gravitational waves (GWs) of different frequencies viz., fundamental (f), pressure (p), rotational (r), spacetime (w), and gravity (g) modes [67]. These modes are classified on the basis of the type of the restoring force that brings the star to equilibrium. For example, in case of the f and p modes, the equilibrium is restored by fluid pressure, while for the g-mode gravity restores the equilibrium. Then the oscillation spectra can be a useful probe to understand the interior and properties of NSs. This is often termed as GW asteroseismology. Among the different frequencies, the most prominent f-mode is of special interest because the future GW detectors such as the *Einstein* Telescope, the *Cosmic Explorer*, and the Laser Interferometer Gravitational Wave Observatory (LIGO) fourth observation (O4) run are being specially designed to match the value of f-mode frequency (1–3 kHz). Therefore, it may be expected that the f-mode frequency of GWs will be detected by these upcoming GW detectors. This will improve our understanding regarding the interior of a NS and its composition and also for further constraining the equation of state (EOS) of NSs. Moreover, universal relations between the f-mode and compactness [68], moment of inertia [69], and static tidal polarizability [70,71] have been obtained for NSs and quark stars, and hybrid stars [72] have emerged due to well correlation between the f-mode and these properties of compact stars. However, p-modes show very weak correlation with such NS properties [68]. Also, the f-mode values are not much affected by the crust [73,74], while the p-mode is sensitive to the low-density crustal EOS [75]. The estimation of the gravitational-radiation flux from NSs thus requires the theory of nonradial oscillations. The nonradial oscillation of the NS was first developed in the framework of general relativity in [76], while the first integrated numerical solution of the NS oscillation was derived in [77]. Later, the method was simplified with the help of Cowling approximations [78] by neglecting the metric perturbations in [79]. The calculation of the oscillation frequencies in full general relativity (GR) conditions that include the spacetime oscillation also give us the opportunity to calculate the w-mode frequency along with the f and p mode frequencies. However, the gross qualitative results remain unaffected, although, the magnitude of frequencies in the Cowling approximation differ from those in the total GR calculations (without Cowling approximation) by up to 30% for the f-mode and ∼15% for p_1-mode [75]. A lot of studies have been done on these different oscillation modes [58,72,80–87]. Only a few of them [58,84,87,88] particularly focused on the nonradial f-mode oscillations of DMANSs and [88] used the bound on tidal deformability from GW data in order to extract the DM composition of the star for the extracted range of f-mode values. However, interaction between DM and NS matter is not considered in [88], and therefore, unlike the present work, they have considered the two-fluid approach to obtain the structural properties of the DMANSs.

In the present work we intend to show how the presence of DM and its interaction with hadronic matter affects the most prominent f-mode frequency of the oscillation of the NSs. For this purpose we consider four well-known RMF

models, viz., NL3 [89], GM1 [90], DD2 [91], and DD-ME2 [92], to describe the hadronic matter content of the star. Within a range of constant DM Fermi momentum k_F^χ, we have already obtained the suitable range of m_χ required to obtain reasonable DMANS configurations with these four hadronic models [1]. Therefore, we use the same in the present work in order to study the effects of the presence of DM on the f-mode oscillation of the DMANSs in terms of m_χ corresponding to constant k_F^χ or constant ρ_χ.

We organize the present work as follows. In the Sec. II, we briefly address the mechanism of invoking feeble interaction of DM with hadronic matter via the dark mediators ϕ and ξ using the four RMF hadronic models NL3, GM1, DD2, and DD-ME2. We also discuss the methodology of estimating the structural properties like mass, radius, tidal deformability, and the f-mode oscillation of the DMANSs. We then present the results of our estimations based on Sec. II and corresponding discussions in Sec. III. We summarize and conclude in the final section, Sec. IV, of the paper.

II. FORMALISM

A. Dark matter admixed neutron star models

For the β-equilibrated hadronic NS matter we consider four well-known RMF models. Of them, NL3 [89] and GM1 [90] are with nonlinear self-couplings, while DD2 [91] and DD-ME2 [92] have density-dependent couplings following the Typel-Wolter ansatz [93]. The values of the couplings and the saturation properties of all four hadronic models considered in this present work can be found in the respective references and also in [94]. In [1] we already invoked feeble DM interaction with hadronic matter using these four RMF models. A phenomenological treatment was considered to describe the self-interaction of nonrelativistic DM by a Yukawa potential [95]. The interaction of the dark fermion (χ) with the hadronic matter ($\psi = \mathrm{n}, \mathrm{p}$) is mediated by the scalar (ϕ) and vector (ξ) new physics mediators. ϕ and ξ interact with the hadronic matter ψ with a very feeble coupling strength $g_\phi = g_\xi \sim 10^{-4}$. Also, ϕ and ξ have their respective couplings with χ as y_ϕ and y_ξ. As considered in our previous works [34,35,96], the values of m_χ, m_ϕ, and m_ξ are consistent with the self-interaction constraints from the Bullet cluster [95,97–100], while the self-interaction couplings are also chosen by reproducing the observed nonbaryonic relic density [101–103]. The values of m_ϕ and m_ξ corresponding to the range of m_χ are already shown in our previous works [34,35,96]. The DM number density ρ_χ is considered to be constant via constant DM Fermi momentum k_F^χ throughout the radial profile of the star following [1,33–35]. It is assumed that the DM density is 10^{-3} times the baryon density [33]. The detailed methodology for obtaining the EOS, i.e, the energy density ε and pressure P (as functions of baryon density ρ) of DMANSs using these four models, can be found in [1].

It is well known that the crust of the NS plays an important role in determining the overall radius of the NS. In our earlier works [1,34,35], and thus in the present work, we have considered constant number density of DM along the radius profile of the star following [33]. This consideration also implies that DM should also be present in the crust although several works on DMANSs have not considered the presence of DM in the crust [104,105]. The methodology adopted for invoking DM interaction with the NS matter in our earlier [1,34,35] and present works requires a Lagrangian formulation of the DMANS matter. For consistency between core and crust, we require a Lagrangian formulation of the crust matter of the NS in order to obtain DM admixed crust EOS, including the interaction between DM and NS crust matter through dark mediators. However, this Lagrangian formulation of the crust matter of the NS is not very common in the present literature. Therefore, the calculation of the DM admixed EOS for the crust is somewhat not easy and beyond the scope of this present work. Therefore, we consider DM interaction only in the core and obtain the DMANS EOS for the core.

B. Structural properties of dark matter admixed neutron stars

Using the DMANS EOS, we estimate the structural properties like the gravitational mass (M) and the radius (R) of the DMANSs. The metric for a spherically symmetric star in static conditions is given as

$$ds^2 = -e^{2\Phi(r)}dt^2 + e^{2\Lambda(r)}dr^2 + r^2d\theta^2 + r^2\sin^2\theta d\phi^2. \quad (1)$$

Based on this metric, the Tolman-Oppenheimer-Volkoff (TOV) equations are derived [106,107] as

$$\frac{dP(r)}{dr} = -(\varepsilon(r) + P(r))\frac{d\Phi(r)}{dr} \quad (2)$$

$$\frac{d\Phi(r)}{dr} = \frac{M(r) + 4\pi r^3 P(r)}{r(r - 2M(r))} \quad (3)$$

$$\frac{dM(r)}{dr} = 4\pi r^2 \varepsilon(r), \quad (4)$$

where $\Phi(r)$ and $\Lambda(r)$ are metric functions with respect to r. The mass function $M(r) = r(1 - e^{-2\Lambda(r)})/2$ satisfies Eq. (4).

These Eqs. (2)–(4) signify the hydrostatic equilibrium between gravity and the internal pressure of the star.

The methodology to calculate the nonradial oscillations of the NSs using the Cowling approximations is well depicted in [79]. Once we obtain the mass and radius of the star by solving the TOV Eqs. (2)–(4), the two following

coupled differential equations are solved to obtain the oscillation mode frequencies:

$$\frac{dW(r)}{dr} = \frac{d\varepsilon(r)}{dP(r)}\left[\omega^2 r^2 e^{\Lambda(r)-2\Phi(r)}V(r) + \frac{d\Phi(r)}{dr}W(r)\right] - l(l+1)e^{\Lambda(r)}V(r) \quad (5)$$

and

$$\frac{dV(r)}{dr} = 2\frac{d\Phi(r)}{dr}V(r) - e^{\Lambda(r)}\frac{W(r)}{r^2}. \quad (6)$$

For the fundamental (f) mode, $l = 2$. Equations (5) and (6) need to be solved by imposing certain boundary

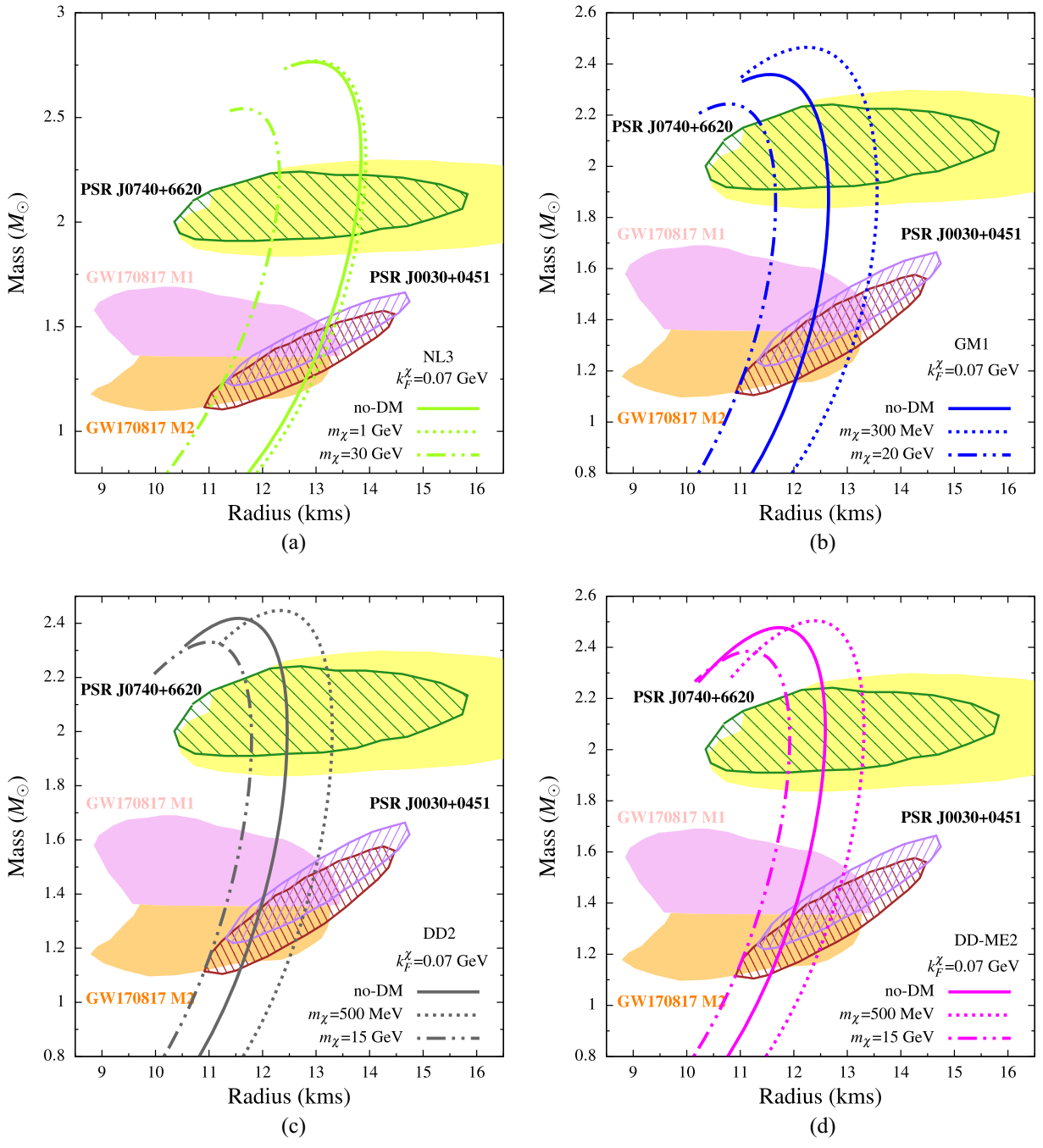


FIG. 1. Variation of mass with radius of neutron stars with and without dark matter for $k_F^\chi = 0.07$ GeV and different hadronic models (a) NL3, (b) GM1, (c) DD2, and (d) DD-ME2. The observational limits imposed from the most massive pulsar PSR J0740 + 6620 ($M = 2.08 \pm 0.07 M_\odot$) [61] and $R = 13.7^{+2.6}_{-1.5}$ km [62] or $R = 12.39^{+1.30}_{-0.98}$ km [63] are also indicated. The constraints on M-R plane prescribed from GW170817 [64] and the NICER experiment for PSR J0030 + 0451 [65,66] are also compared.

conditions at the center ($r = 0$) and the surface ($r = R$) of the star. At $r = 0$ the functions $W(r)$ and $V(r)$ behave as

$$W(r) = Cr^{l+1} \quad \text{and} \quad V(r) = -Cr^{l}/l, \tag{7}$$

and at $r = R$ with vanishing perturbation the boundary condition of $W(r)$ and $V(r)$ is in the form of

$$\omega^2 r^2 e^{\Lambda(R)-2\Phi(R)} V(R) + \left.\frac{d\Phi(r)}{dr}\right|_{r=R} W(R) = 0. \tag{8}$$

The coupled differential equations, Eqs. (5) and (6), are integrated from the center to the surface of the star by considering an initial value of ω^2. The value of ω^2 is improved after each integration with the help of the Ridder's method until Eq. (8) is satisfied.

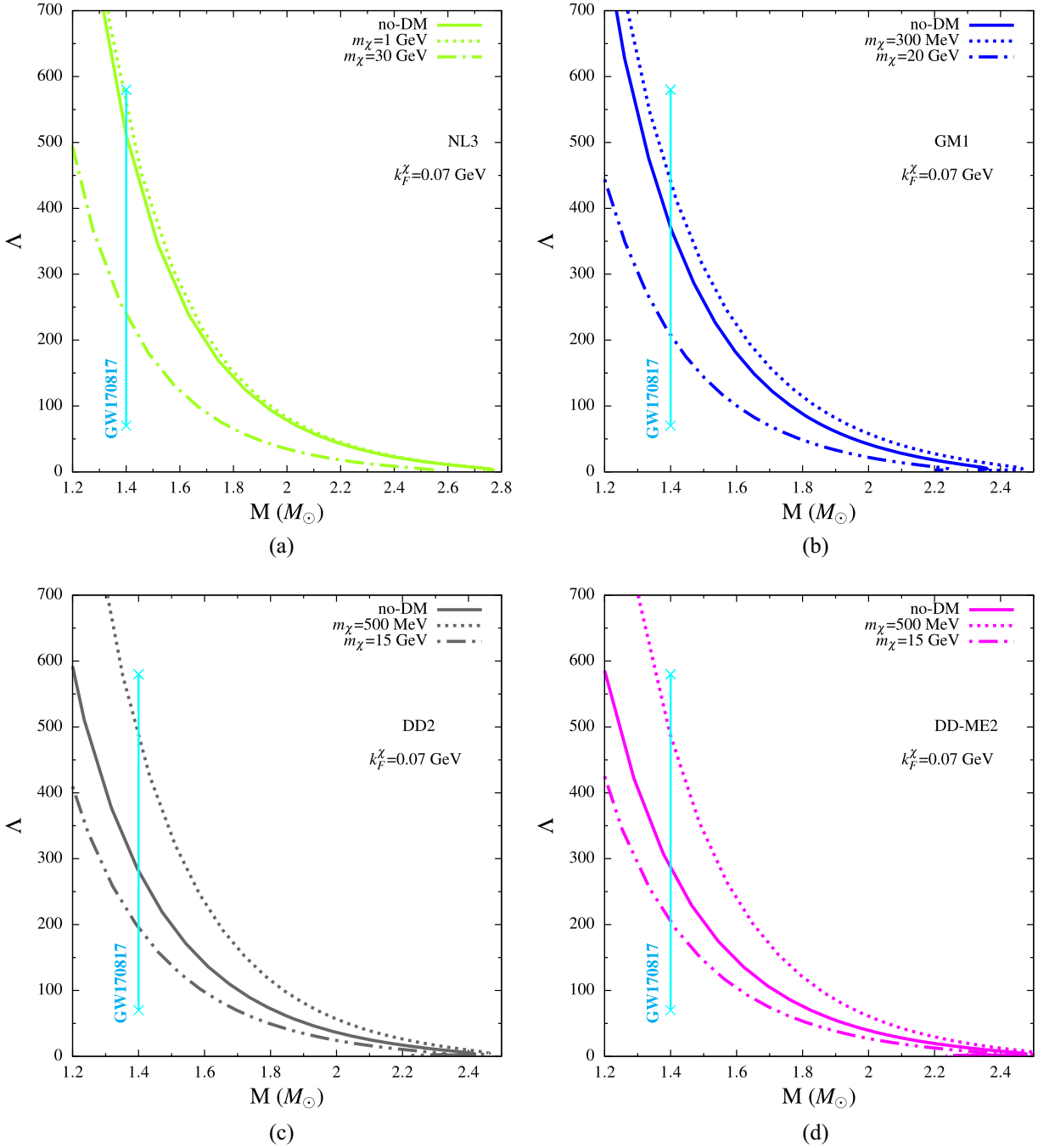


FIG. 2. Variation of tidal deformability with the mass of neutron stars with and without dark matter for $k_F^\chi = 0.07$ GeV and different hadronic models (a) NL3, (b) GM1, (c) DD2, and (d) DD-ME2. The constraint on $\Lambda_{1.4}$ from GW170817 [64] is also shown.

The dimensionless tidal deformability (Λ) is obtained in terms of the mass, radius, and the tidal love number (k_2), following [108,109].

III. RESULTS

In [1] we obtained the suitable range of m_χ, corresponding to the range of $k_F^\chi = (0.01\text{–}0.07)$ GeV, that can yield reasonable DMANS configurations, in terms of the various astrophysical constraints on the structural properties of NSs. For the four hadronic models considered in this work, the range of m_χ is as follows:

$$\text{NL3}: m_\chi = (1\text{–}30)\ \text{GeV}$$
$$\text{GM1}: m_\chi = (0.3\text{–}20)\ \text{GeV}$$
$$\text{DD2}: m_\chi = (0.5\text{–}15)\ \text{GeV}$$
$$\text{DD-ME2}: m_\chi = (0.5\text{–}15)\ \text{GeV}$$

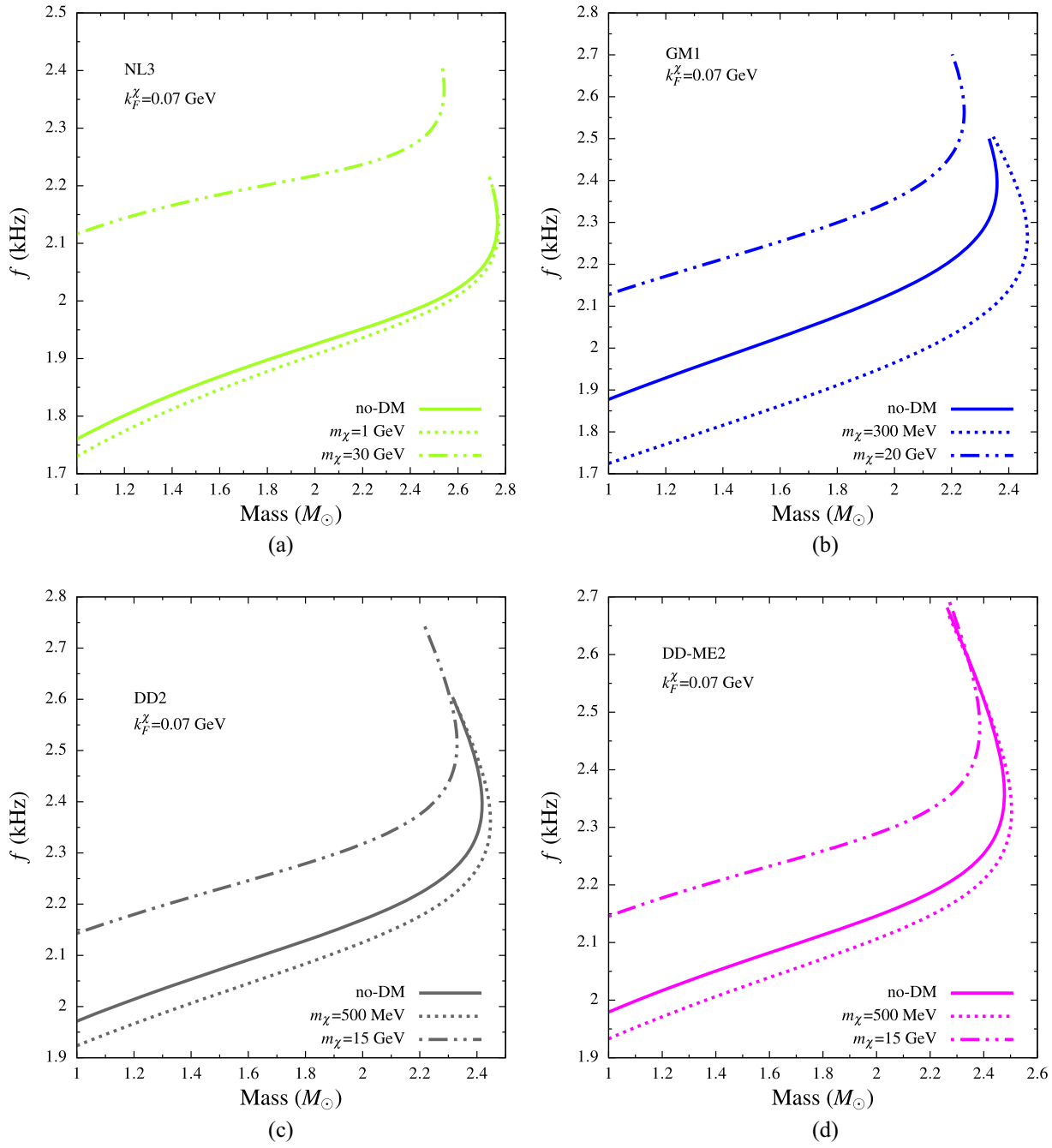


FIG. 3. Variation of f-mode frequency with the mass of neutron stars with and without dark matter for $k_F^\chi = 0.07$ GeV and different hadronic models (a) NL3, (b) GM1, (c) DD2, and (d) DD-ME2.

TABLE I. The values of f_{ll}^{DMANS} and f_{ul}^{DMANS} for dark matter admixed neutron stars with corresponding M_{ll}^{DMANS} and M_{ul}^{DMANS} and m_χ^{min} and m_χ^{max} for $k_F^\chi = 0.07$ GeV.

Model	m_χ^{min} (GeV)	M_{ul}^{DMANS} ($M_\odot$)	f_{ll}^{DMANS} (kHz)	m_χ^{max} (GeV)	M_{ll}^{DMANS} ($M_\odot$)	f_{ul}^{DMANS} (kHz)
NL3	1	2.77	2.13	30	2.54	2.36
GM1	0.3	2.46	2.26	20	2.24	2.56
DD2	0.5	2.45	2.36	15	2.33	2.52
DD-ME2	0.5	2.50	2.33	15	2.38	2.47

We first show the structural properties like mass, radius, tidal deformability, and then the f-mode frequency of the DMANSs considering $k_F^\chi = 0.07$ GeV for the range of m_χ corresponding to each hadronic model.

In Figs. (1) and (2) we display the variation of mass with respect to radius and the relationship of the tidal deformability with the mass of DMANSs. We have also compared the case of pure hadronic stars, i.e, the no-DM scenario. The presence of massive DM lowers both the maximum mass and radius of the star. For $k_F^\chi = 0.07$ GeV and for each hadronic model, the maximum and minimum values of m_χ are obtained for which all the constraints on the M-R and Λ-M planes are satisfied. For example, for the GM1 model, values of m_χ below 300 MeV do not satisfy the GW170817 data, while $m_\chi > 20$ GeV fails to satisfy the NICER experiment for PSR J0030 + 0451.

We next present in Fig. (3) the dependence of the f-mode frequency on the mass of NSs without DM and with DM considering the fixed values of k_F^χ and m_χ, respective to each hadronic model. The f-mode frequency increases with the mass of the star. Beyond the maximum mass M_{max} of the star, the value of f keeps increasing further. However, beyond M_{max}, the $M - R$ variation is unstable. Therefore, the values of f in this region are not important, and we consider f_{max} as the value of f corresponding to M_{max}. In the "no-DM" scenario, the obtained values of f_{max} in the present work are consistent with that obtained in [80] for the NL3 and GM1 models and [83] for the NL3, GM1, and DD2 models. For instance, in case of the GM1 model, we find from Fig. 3(b) that in the no-DM scenario $f_{\mathrm{max}} = 2.39$ kHz corresponding to $M_{\mathrm{max}} = 2.36 M_\odot$, but while in presence of DM, $f_{\mathrm{max}} = 2.26$ and 2.56 kHz corresponding to $M_{\mathrm{max}} = 2.46$ and $2.24 M_\odot$ for $m_\chi = 300$ MeV and 20 GeV, respectively. This also implies that the presence of DM has pronounced effects on the f whose value is higher in the case of massive DM. The value of f depends on both the mass and radius of the DMANSs, which are, in turn, dictated by m_χ via the DM admixed EOS. Note that f not only depends on the mass of the star but also on its radius. For example, in case of the NL3 model, we find from Fig. 1(a) that there is negligible difference in maximum mass of the star between the no-DM scenario and the case when $m_\chi = 30$ GeV. The difference in radius between the two scenarios is also quite small, especially in the high mass region. The same effect is reflected in the behavior of f in Fig. 3(a) where the value of f, corresponding to the maximum mass of the star, is almost equal to the no-DM case and for $m_\chi = 30$ GeV. There is, however, noticeable difference in the value of f for the two scenarios at low mass regime, which is a reflection of the behavior of radius in this regime.

Now for any particular hadronic model, the upper and the lower limits of m_χ are fixed for $k_F^\chi = (0.01\text{–}0.07)$ GeV [1]. This implies that in the presence of DM with a fixed k_F^χ, the range of maximum mass configurations of the DMANSs is also fixed. The lower values of m_χ produces more massive DMANSs with respect to the radius as seen from Fig. (1). Consequently, the maximum mass of the DMANS for a given model becomes higher for the lower values of m_χ. Therefore, m_χ^{max} for any model produces DMANS with the lowest value of the maximum mass for that model in the range $k_F^\chi = (0.01\text{–}0.07)$ GeV. Let us denote this lowest value of the maximum mass as M_{ll}^{DMANS}. Similarly, m_χ^{min} yields DMANS with the highest value of the maximum mass for that model. We denote this highest value of the maximum mass as M_{ul}^{DMANS}. For example, for the GM1 model $m_\chi^{\mathrm{max}} = 20$ GeV gives $M_{ll}^{\mathrm{DMANS}} = 2.24 M_\odot$, while $M_{ul}^{\mathrm{DMANS}} = 2.46$ for $m_\chi^{\mathrm{min}} = 300$ MeV. Consequently, in the presence of DM, the upper and the lower limits of f_{max} (f corresponding to M_{max}) are also fixed for any particular model. Now, contrary to the values of the maximum mass of DMANSs, it is seen from Fig. (3) that massive DM gives rise to higher values of f_{max}, i.e., m_χ^{max} for any model gives the upper limit of the f_{max}, while m_χ^{min} produces the lower limit of f_{max} for a fixed model. We denote the upper limit of f_{max} as f_{ul}^{DMANS} produced by m_χ^{max} and the lower limit of f_{max} as f_{ll}^{DMANS} given by m_χ^{min}. As an example for the GM1 model, $m_\chi^{\mathrm{max}} = 20$ GeV gives $f_{ul}^{\mathrm{DMANS}} = 2.56$ kHz, while for $m_\chi^{\mathrm{min}} = 300$ MeV, $f_{ll}^{\mathrm{DMANS}} = 2.26$ kHz. Therefore, in Table I, we show the values of f_{ul}^{DMANS} and f_{ll}^{DMANS} corresponding to M_{ll}^{DMANS} and M_{ul}^{DMANS} with m_χ^{max} and m_χ^{min}, respectively.

Considering all four hadronic models, we find that the common allowed range of m_χ is (1–15) GeV. Therefore, within this m_χ and fixed $k_F^\chi = 0.07$ GeV, we next compare in Fig. (4) the values of $f_{1.4}$ and $f_{2.01}$ for the DMANSs

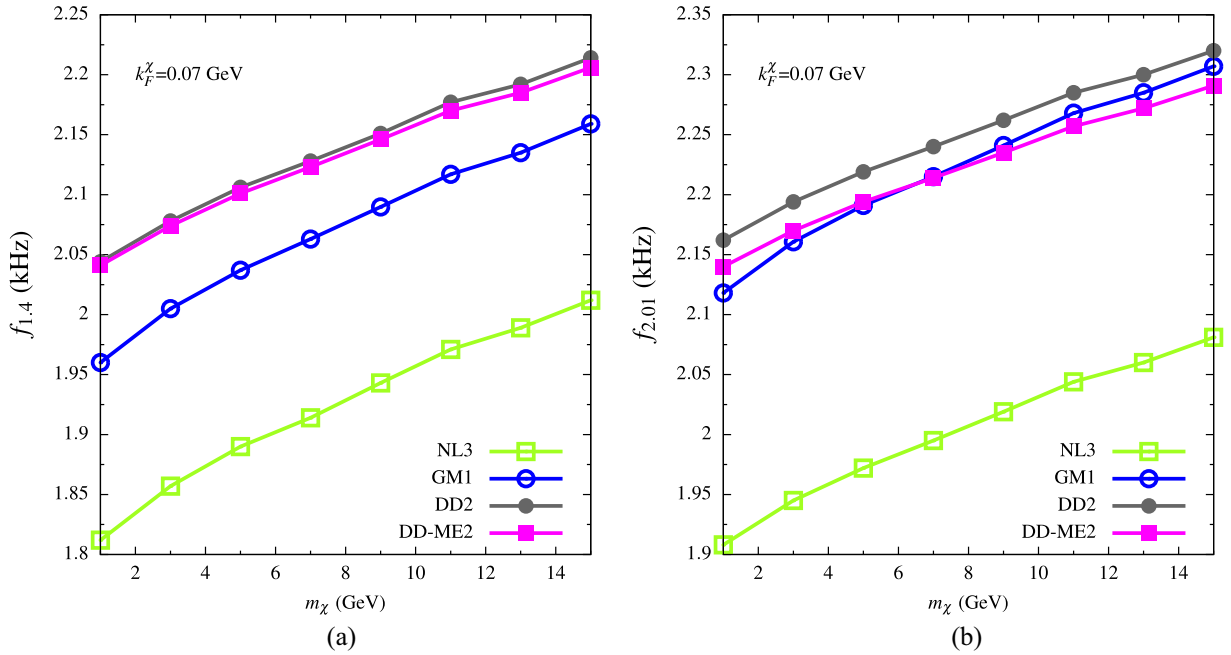


FIG. 4. Variation of (a) $f_{1.4}$ and (b) $f_{2.01}$ with the mass of fermionic dark matter for $k_F^\chi = 0.07$ GeV compared for different hadronic models.

obtained with the different hadronic models. $f_{1.4}$ and $f_{2.01}$ are the values of f corresponding to the DMANSs of mass $1.4M_\odot$ and $2.01M_\odot$, respectively. These values are important because one of the binary components associated with GW170817 has a mass of $1.4M_\odot$ while the lower limit of mass of the most massive pulsar PSR J0740 + 6620, detected to date, is $2.01M_\odot$. The underlying RMF EOS plays a role in deciding the magnitude of f-mode. For example, for any particular value of m_χ and k_F^χ, Fig. 4(a) shows that the value of $f_{1.4}$, in terms of the model, follows the sequence NL3 < GM1 < DD-ME2 < DD2. Since a $1.4M_\odot$ is obtained at low values of density, we find that at lower density the stiffness of the EOS in the no-DM scenario follows the reverse trend as NL3 < GM1 < DD-ME2 < DD2. Thus it can be said that stiffer EOS results in $f_{1.4}$ of lower magnitude. As expected, both $f_{1.4}$

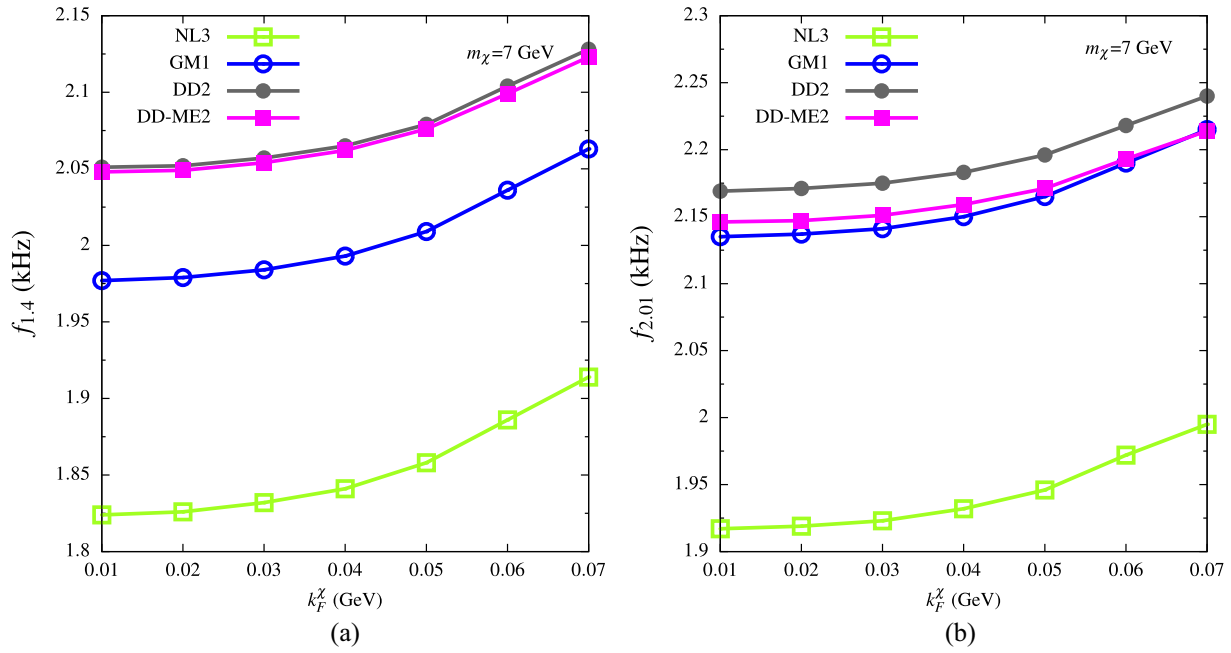


FIG. 5. Variation of (a) $f_{1.4}$ and (b) $f_{2.01}$ with constant Fermi momentum of dark matter for $m_\chi = 7$ GeV compared for different hadronic models.

and $f_{2.01}$ increase with m_χ for all the models. Figures 4(a) and 4(b) show that for any value of m_χ, the values of both $f_{1.4}$ and $f_{2.01}$ are minimum for NL3 and maximum for DD2. This is because the values of $R_{1.4}$ and $R_{2.01}$ are maximum for NL3 and minimum for DD2. The values of both $f_{1.4}$ and $f_{2.01}$ are almost the same for DD2 and DD-ME2 models for any value of m_χ.

The common range of $m_\chi = (1\text{–}15)$ GeV is not only valid for $k_F^\chi = 0.07$ GeV but within a range of $k_F^\chi = (0.01\text{–}0.07)$ GeV, as we obtained in [1]. Therefore, in Fig. 5 we now study the variation of $f_{1.4}$ and $f_{2.01}$ with respect to k_F^χ in the range of (0.01–0.07) GeV for a fixed value of $m_\chi = 7$ GeV that falls within the acceptable common range of $m_\chi = (1\text{–}15)$ GeV. The dependence of $f_{1.4}$ and $f_{2.01}$ on k_F^χ is compared for all four hadronic models. The values of $f_{1.4}$ and $f_{2.01}$ increase with k_F^χ and, similar to Fig. (4), the values of $f_{1.4}$ and $f_{2.01}$ are maximum for the DD2 model and minimum for NL3 for any particular value of m_χ. Interestingly, from Figs. 4 and 5 we observe that the variation of $f_{1.4}$ with both m_χ [Fig. 4(a)] and k_F^χ [Fig. 5(a)] are obtained parallel for all four hadronic models, while in the case of variation of $f_{2.01}$ the curves for the GM1 and DD-ME2 models intersect and overlap.

We finally try to understand the complete effect of the presence of DM on the values of $f_{1.4}$ and $f_{2.01}$ for the four individual hadronic models NL3, GM1, DD2, and DD-ME2 in Figs. 6, 7, 8, and 9, respectively. The complete effect of DM can be seen from the combined effect of m_χ and k_F^χ, which is studied in these figures. We span the common allowed range of $m_\chi = (1\text{–}15)$ GeV fully and also the total range of $k_F^\chi = (0.01\text{–}0.07)$ GeV in the following figures. Figures 6(a), 6(b), 7(a), 7(b), 8(a), 8(b), 9(a), and 9(b) show that for any particular hadronic model

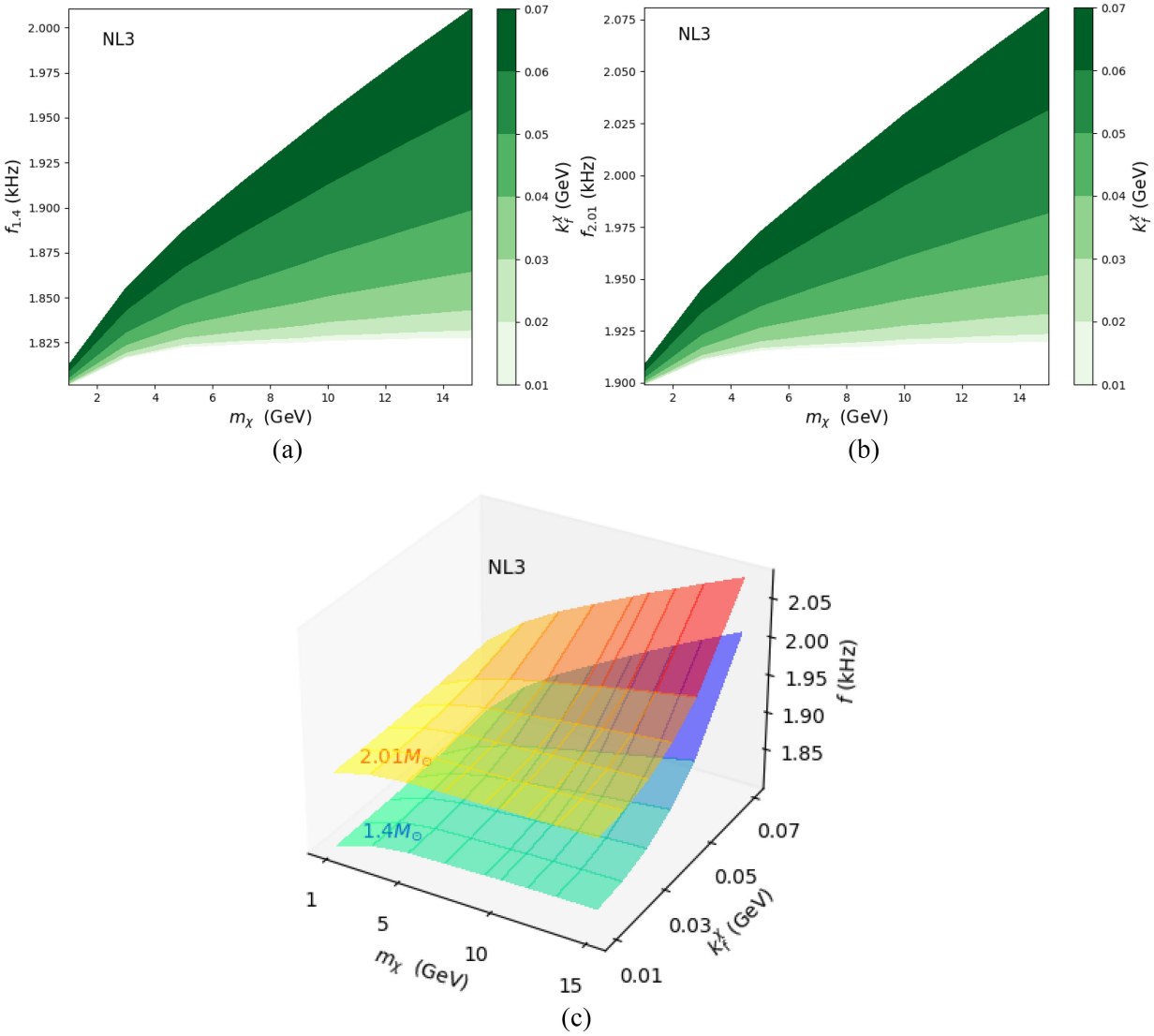


FIG. 6. Variation of (a) $f_{1.4}$ and (b) $f_{2.01}$ with m_χ and k_F^χ with NL3 hadronic model. (c) Corresponding consolidated 3-dimensional variation.

$f_{1.4}$ and $f_{2.01}$ increase with m_χ. This increasing behavior is further escalated with the larger values of k_F^χ.

Each band represents the variation of $f_{1.4}$ and/or $f_{2.01}$ with respect to m_χ for the value of k_F^χ within an interval of 0.01 GeV. The interface of any two consecutive bands represents $f_{1.4}$ and/or $f_{2.01}$ with respect to m_χ for a fixed value of k_F^χ, which is denoted in the color bar. It is interesting to note that for decreasing k_F^χ there is monotonic squeezing of the bands. This is because at very low k_F^χ, the DM population in terms of DM mass density ρ_χ is too low, irrespective of m_χ. Under such circumstances, the findings related to the structural properties of the star are very similar to that of the no-DM scenario, as also seen in [1]. For example, for the DD-ME2 model, the values of $f_{1.4}$ and $f_{2.01}$ for $k_F^\chi = 0.01$ GeV are approximately 2.05 and 2.15 kHz, respectively, as seen from Figs. 9(a) and 9(b). These values of $f_{1.4}$ and $f_{2.01}$ are very close to that obtained in the no-DM scenario for the DD-ME2 model as seen from Fig. 3(d).

In Figs. 6(c), 7(c), 8(c), and 9(c) we depict the 3-dimensional representation of the variation of $f_{1.4}$ and $f_{2.01}$ with respect to both m_χ and k_F^χ. In such representation, we obtain the values of $f_{1.4}$ and $f_{2.01}$ as two separate non-overlapping planes. From Figs. 6–9 we also provide the range of $f_{1.4}$ and $f_{2.01}$ of the DMANSs for the accepted range of m_χ, corresponding to the range of k_F^χ. For example, for the DD2 model, $f_{1.4}^{\rm DMANS} = (2.03\text{–}2.16)$ kHz and $f_{2.01}^{\rm DMANS} = (2.15\text{–}2.32)$ kHz.

We calculate the p_1-mode frequency of the NSs without DM and with DM considering the fixed value of $k_F^\chi = 0.07$ GeV. For DMANSs we choose to work with the maximum and minimum values of m_χ respective to different hadronic models. In case of the p-mode, $l = 2$, similar to the f-mode scenario. However, the number of

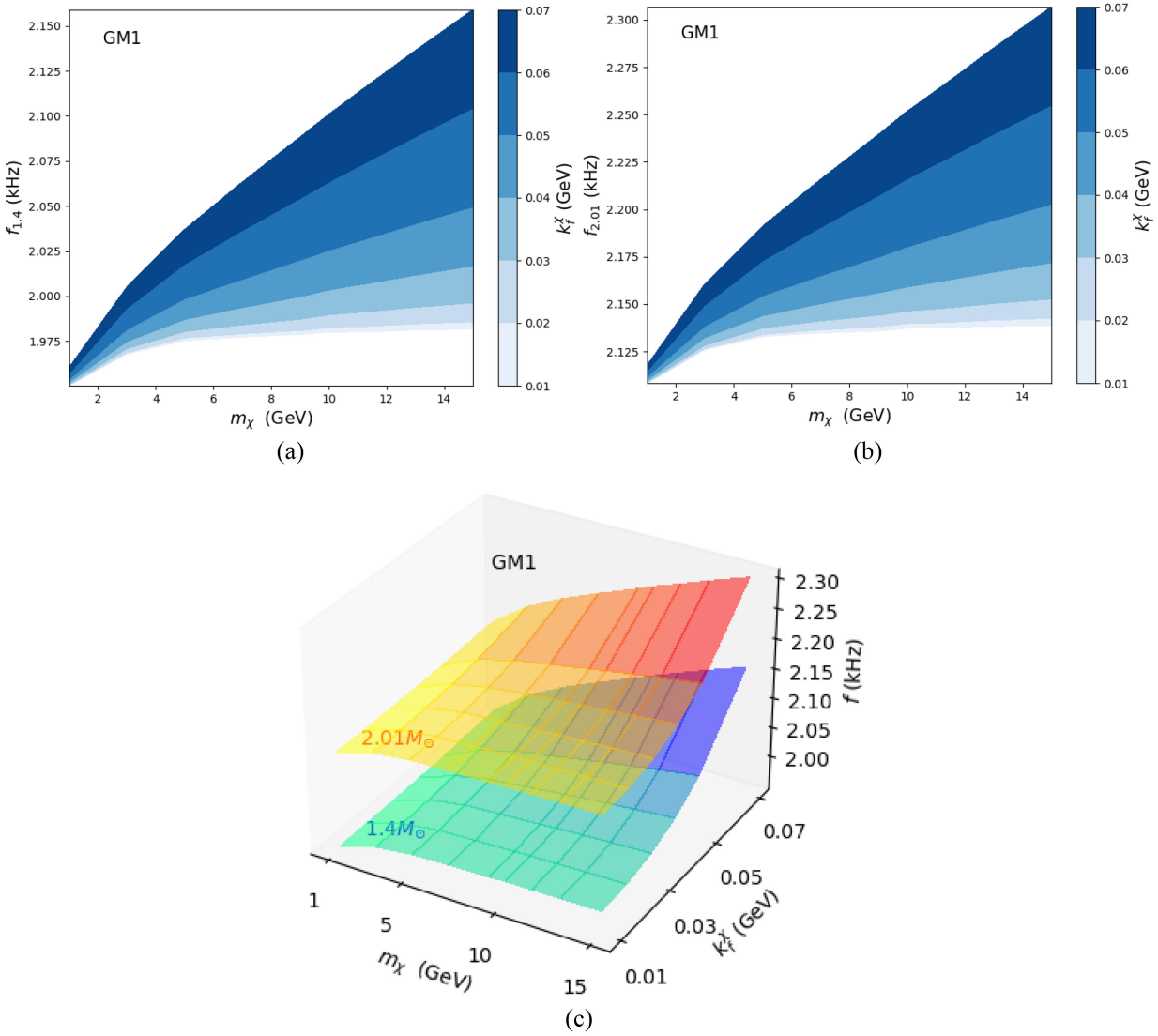


FIG. 7. Variation of (a) $f_{1.4}$ and (b) $f_{2.01}$ with m_χ and k_F^χ with GM1 hadronic model. (c) Corresponding consolidated 3-dimensional variation.

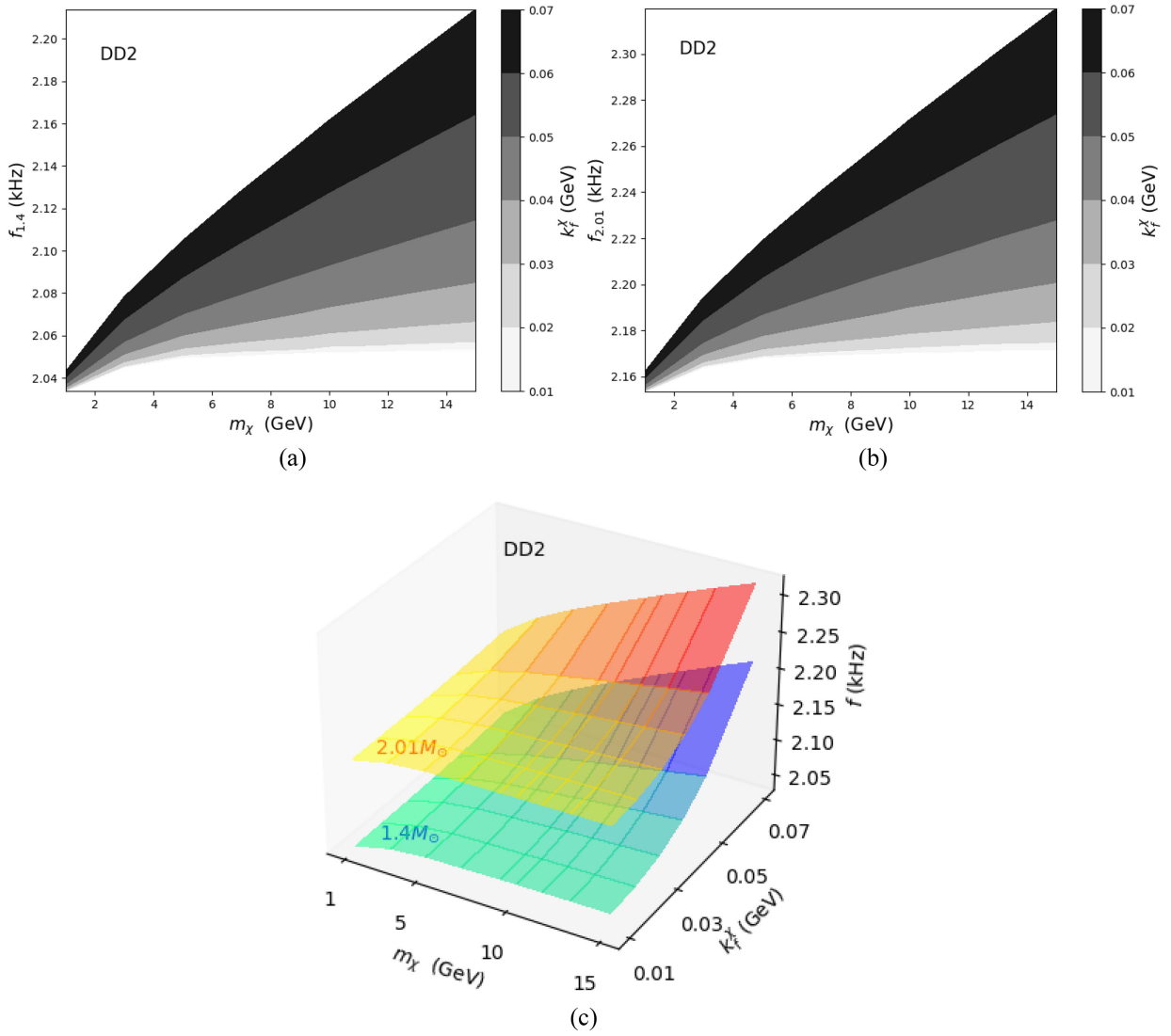


FIG. 8. Variation of (a) $f_{1.4}$ and (b) $f_{2.01}$ with m_χ and k_F^χ with DD2 hadronic model. (c) Corresponding consolidated 3-dimensional variation.

nodes for the p-mode is $n = 1$, unlike the f-mode which has no node. In Fig. 10 we show the variation of the p_1-mode frequency with respect to the mass of the of NSs with and without DM for the two hadronic models NL3 [Fig. 10(a)] and DD2 [Fig. 10(b)]. We know that unlike the f-mode frequencies, which are not much affected by the crust [73,74,110,111], the p-mode is quite sensitive to the low-density crustal EoS [75]. As stated earlier that we have not considered the crustal effects of the NSs. Therefore, our results of the magnitude of the p_1-mode frequency of the NSs without DM are different (a bit larger) than that obtained in [80,83] especially at low mass (density). However, the value of p_{1max} (corresponding to M_{max}) do not differ much from that obtained in [80,83] as the deviation is noticed only at the second significant figure. In the present work we obtain the values of p_{1max} for the NSs without DM as 6.08 kHz for NL3 model and 6.66 kHz for the DD2 model while in [80] p_{1max} is obtained as ∼6 kHz for the NL3 model and in [83] the value of p_{1max} is ∼6.5 kHz. It is observed from both the Figs. 10(a) and 10(b) that for the cases of no-DM and the DMANSs with minimum value of m_χ, the $p_1 - M$ variation initially follows a flat or slightly increasing trend that decreases after a certain value of mass (density). For the maximum value of m_χ, the variation of p_1 shows an overall decreasing trend along the mass (density) profile of the star. In the present work we obtain the range of p_{1max}^{DMANS} as (6.03–6.94) kHz for the NL3 model and (6.49–7.04) kHz for the DD2 model.

IV. SUMMARY AND CONCLUSION

The feeble interaction between the fermionic DM (χ) with the hadronic matter is introduced through a dark scalar (ϕ) and a dark vector (ξ) boson as mediators in [1], where m_χ is

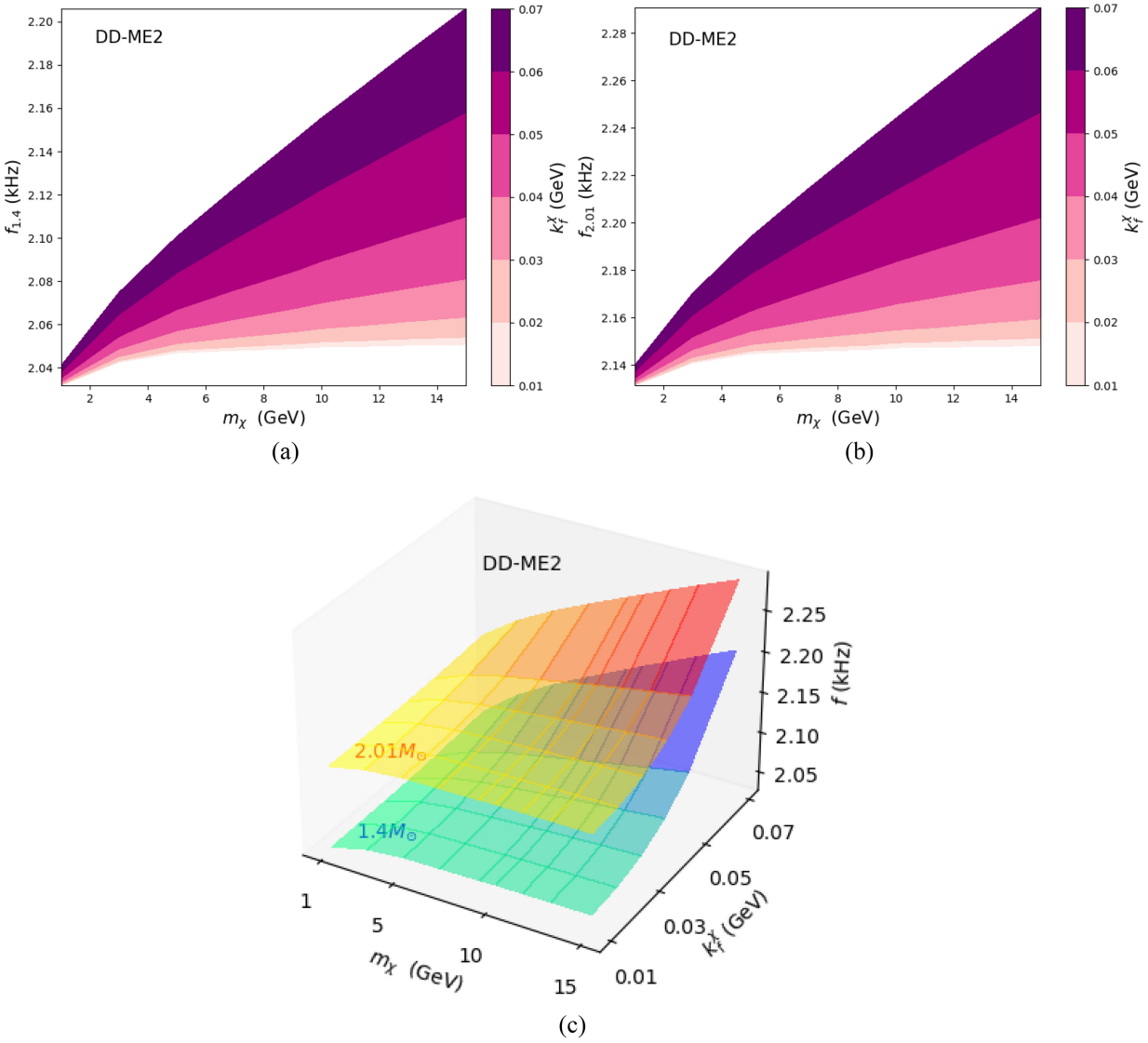


FIG. 9. Variation of (a) $f_{1.4}$ and (b) $f_{2.01}$ with m_χ and k_F^χ with DD-ME2 hadronic model. (c) Corresponding consolidated 3-dimensional variation.

related to m_ϕ and m_ξ via the constraint from the Bullet cluster, while the coupling strengths of ϕ and ξ with χ are obtained using the bound from the present day relic abundance. In the same paper, we prescribed for different hadronic models, the allowed range of m_χ that can help the DMANS configurations to satisfy all the observational and astrophysical constraints on the structural properties like the mass, radius, and tidal deformability of compact stars.

In the present work, we utilize the allowed range of m_χ to study the effects of such feeble interaction of DM with the hadronic star matter on the nonradial f-mode oscillation of the DMANSs considering the Cowling approximation. In terms of m_χ and k_F^χ, we found that DM has profound influence in determining the f-mode frequency of NS oscillation. For a fixed value of k_F^χ, we also determined the possible range of $f^{\rm DMANS}$ corresponding to that of m_χ for four particular hadronic RMF models. For instance, we obtain for $k_F^\chi = 0.07$ GeV the range of $f^{\rm DMANS}$ for the following hadronic models as follows:

$$\begin{aligned}
\text{NL3}&: f_{\rm max}^{\rm DMANS} = (2.13\text{–}2.36)\ \text{kHz}\\
\text{GM1}&: f_{\rm max}^{\rm DMANS} = (2.26\text{–}2.56)\ \text{kHz}\\
\text{DD2}&: f_{\rm max}^{\rm DMANS} = (2.36\text{–}2.52)\ \text{kHz}\\
\text{DD-ME2}&: f_{\rm max}^{\rm DMANS} = (2.33\text{–}2.47)\ \text{kHz}
\end{aligned}$$

So in the framework of our DMANSs in the present work, the range of $f_{\rm max}^{\rm DMANS} = (2.13\text{–}2.56)$ kHz considering all four hadronic models.

Since the properties of 1.4 and $2.01M_\odot$ are of current interest, we particularly studied both the individual and combined dependence of $f_{1.4}$ and $f_{2.01}$ on both m_χ and k_F^χ. We found that the variation of $f_{1.4}$ and $f_{2.01}$ increases with m_χ, which is further boosted by large

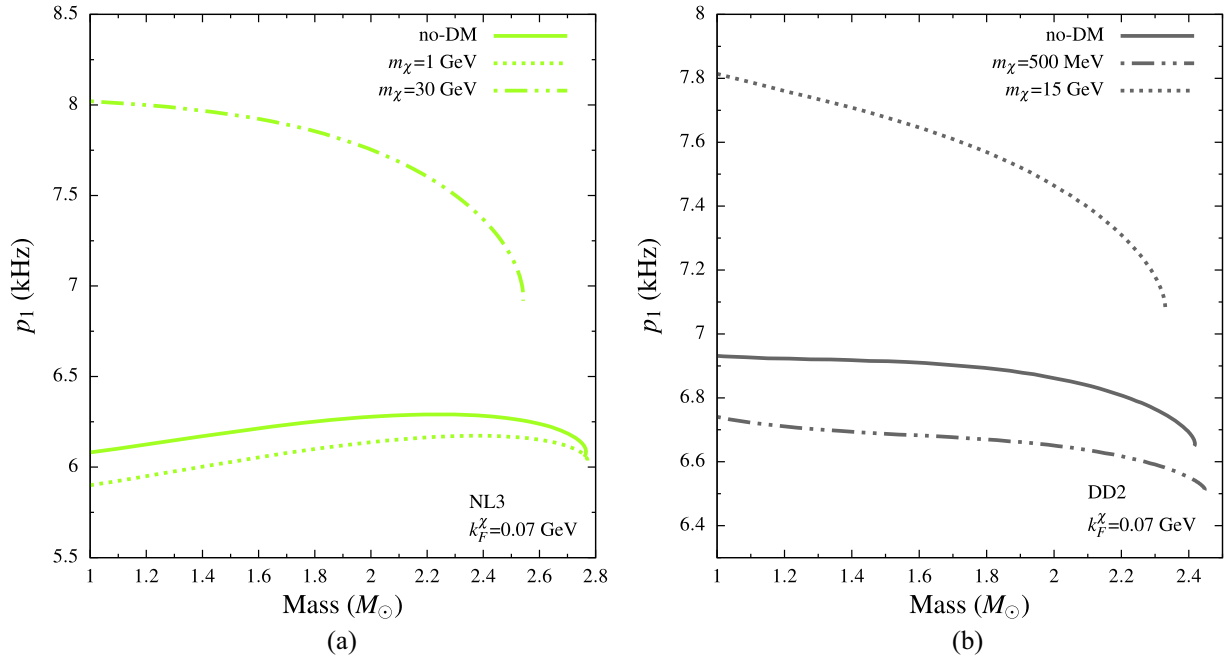


FIG. 10. Variation of p_1-mode frequency with the mass of neutron stars with and without dark matter for $k_F^\chi = 0.07$ GeV and different hadronic models (a) NL3 and (b) DD2.

values of k_F^χ. For the four hadronic models, the range of $f_{1.4}$ and $f_{2.01}$ of DMANSs with respect to the acceptable range of m_χ corresponding to the range of k_F^χ is tabulated below:

$$\begin{aligned}
\text{NL3}&: f_{1.4}^{\text{DMANS}} = (1.80\text{–}1.95)\ \text{kHz}\\
\text{GM1}&: f_{1.4}^{\text{DMANS}} = (1.95\text{–}2.16)\ \text{kHz}\\
\text{DD2}&: f_{1.4}^{\text{DMANS}} = (2.03\text{–}2.16)\ \text{kHz}\\
\text{DD-ME2}&: f_{1.4}^{\text{DMANS}} = (2.03\text{–}2.20)\ \text{kHz}
\end{aligned}$$

$$\begin{aligned}
\text{NL3}&: f_{2.01}^{\text{DMANS}} = (1.90\text{–}2.08)\ \text{kHz}\\
\text{GM1}&: f_{2.01}^{\text{DMANS}} = (2.11\text{–}2.31)\ \text{kHz}\\
\text{DD2}&: f_{2.01}^{\text{DMANS}} = (2.15\text{–}2.32)\ \text{kHz}\\
\text{DD-ME2}&: f_{2.01}^{\text{DMANS}} = (2.13\text{–}2.29)\ \text{kHz}
\end{aligned}$$

Thus in the present work, considering all four hadronic models, $f_{1.4}^{\text{DMANS}}$ and $f_{2.01}^{\text{DMANS}}$ lie in the range (1.80–2.20) kHz and (1.90–2.32) kHz, respectively.

It should be mentioned that we have not included the effects of the NS crust in [1] while obtaining the range of m_χ, due to the absence of a suitable DM admixed crust EOS. Therefore, in the future if a suitable DM admixed NS crust EOS can be obtained with a technique consistent with that used for obtaining the EOS of the core of the DMANSs, then it can be employed to recalculate the gross properties of the DMANSs. In that case, the range of m_χ (consistent with the various astrophysical constraints) will be modified due to modification in the radii of the DMANSs. Consequently, the range of $f_{\text{max}}^{\text{DMANS}}$, $f_{1.4}^{\text{DMANS}}$, and $f_{2.01}^{\text{DMANS}}$ will be modified according to the modified range of m_χ.

We have also calculated the values of p_1-mode frequency of the NSs with and without DM. We found that in absence of the crustal effects, the values of p_1-mode in the "no-DM" case, are larger than that generally obtained in literature, especially at low density. Unlike the p_1-mode, the effects of the crust EoS is not remarkable on the f-mode of NSs. Therefore, in the present work we mainly focus on the variation and magnitude of the f-mode both in presence and absence of DM. Moreover, f-mode is of special interest because it is the most prominent oscillation frequency and thus compared to the higher order modes, it is more likely to be measured by the upcoming facilities like the *Einstein* Telescope, the Cosmic Explorer, and the LIGO O4 run.

Also, in the present work the nonradial oscillation frequencies like the f and p_1 mode frequencies of the NSs, with and without DM, are calculated in the Cowling approximation neglecting the metric perturbations in spacetime. Therefore, it will be interesting to calculate the oscillation frequencies in full GR conditions that include the spacetime oscillation. Such consideration will also give us the opportunity to calculate the w-mode frequency along with the f and p_1 mode frequencies.

ACKNOWLEDGMENTS

The work of D. S. is supported by the NRF research Grant (No. 2018R1A5A1025563). The work of A. G. is supported by the National Research Foundation of Korea (No. MSIT RS-2024-00356960).

[1] A. Guha and D. Sen, Phys. Rev. D **109**, 043038 (2024).
[2] P. A. R. Ade *et al.* (Planck Collaboration), Astron. Astrophys. **594**, A13 (2016).
[3] G. Bertone, D. Hooper, and J. Silk, Phys. Rep. **405**, 279 (2005).
[4] N. Aghanim *et al.* (Planck Collaboration), Astron. Astrophys. **641**, A6 (2020).
[5] J. B. Bauer, D. J. E. Marsh, R. Hložek, H. Padmanabhan, and A. Laguë, Mon. Not. R. Astron. Soc. **500**, 3162 (2020).
[6] M. Lisanti, in *New Frontiers in Fields and Strings* (World Scientific, Singapore, 2017), pp. 399–446.
[7] S. Profumo, in *Searching for New Physics at Small and Large Scales* (World Scientific, Singapore, 2013), pp. 143–189.
[8] R. Agnese *et al.* (SuperCDMS Collaboration), Phys. Rev. Lett. **121**, 051301 (2018); **122**, 069901(E) (2019).
[9] E. Aprile *et al.* (XENON Collaboration), Phys. Rev. Lett. **129**, 161805 (2022).
[10] Q. Wang *et al.* (PandaX-II Collaboration), Chin. Phys. C **44**, 125001 (2020).
[11] P. Agnes *et al.* (DarkSide Collaboration), Phys. Rev. Lett. **121**, 111303 (2018).
[12] M. Crisler, R. Essig, J. Estrada, G. Fernandez, J. Tiffenberg, M. Sofo haro, T. Volansky, and T.-T. Yu (SENSEI Collaboration), Phys. Rev. Lett. **121**, 061803 (2018).
[13] J. Aalbers *et al.* (LZ Collaboration), Phys. Rev. Lett. **131**, 041002 (2023).
[14] W. B. Atwood *et al.* (Fermi-LAT Collaboration), Astrophys. J. **697**, 1071 (2009).
[15] M. G. Aartsen *et al.* (IceCube Collaboration), Phys. Rev. Lett. **113**, 101101 (2014).
[16] O. Adriani *et al.* (PAMELA Collaboration), Nature (London) **458**, 607 (2009).
[17] O. Adriani *et al.* (PAMELA Collaboration), Phys. Rev. Lett. **111**, 081102 (2013).
[18] L. Accardo *et al.* (AMS Collaboration), Phys. Rev. Lett. **113**, 121101 (2014).
[19] M. Boudaud, J. Lavalle, and P. Salati, Phys. Rev. Lett. **119**, 021103 (2017).
[20] O. Adriani *et al.* (CALET Collaboration), Phys. Rev. Lett. **119**, 181101 (2017).
[21] O. Adriani *et al.*, Phys. Rev. Lett. **120**, 261102 (2018).
[22] M. Baryakhtar, J. Bramante, S. W. Li, T. Linden, and N. Raj, Phys. Rev. Lett. **119**, 131801 (2017).
[23] A. Joglekar, N. Raj, P. Tanedo, and H.-B. Yu, Phys. Lett. B **809**, 135767 (2020).
[24] N. F. Bell, G. Busoni, and S. Robles, J. Cosmol. Astropart. Phys. 06 (2019) 054.
[25] A. Joglekar, N. Raj, P. Tanedo, and H.-B. Yu, Phys. Rev. D **102**, 123002 (2020).
[26] J. Bramante and N. Raj, Phys. Rep. **1052**, 1 (2024).
[27] W. Husain, T. F. Motta, and A. W. Thomas, J. Cosmol. Astropart. Phys. 10 (2022) 028.
[28] W. Husain and A. W. Thomas, J. Phys. G **50**, 015202 (2023).
[29] W. Husain, D. Sengupta, and A. W. Thomas, Universe **9**, 307 (2023).
[30] D. Zhou, Universe **9**, 484 (2023).
[31] A. Nelson, S. Reddy, and D. Zhou, J. Cosmol. Astropart. Phys. 07 (2019) 012.
[32] N. F. Bell, G. Busoni, S. Robles, and M. Virgato, J. Cosmol. Astropart. Phys. 03 (2021) 086.
[33] G. Panotopoulos and I. Lopes, Phys. Rev. D **96**, 083004 (2017).
[34] A. Guha and D. Sen, J. Cosmol. Astropart. Phys. 09 (2021) 027.
[35] D. Sen and A. Guha, Mon. Not. R. Astron. Soc. **504**, 3354 (2021).
[36] S. Shakeri and D. R. Karkevandi, Phys. Rev. D **109**, 043029 (2024).
[37] D. R. Karkevandi, S. Shakeri, V. Sagun, and O. Ivanytskyi, Phys. Rev. D **105**, 023001 (2022).
[38] C. H. Lenzi, M. Dutra, O. Lourenço, L. L. Lopes, and D. P. Menezes, Eur. Phys. J. C **83**, 266 (2023).
[39] O. Lourenço, C. H. Lenzi, T. Frederico, and M. Dutra, Phys. Rev. D **106**, 043010 (2022).
[40] I. Lopes and G. Panotopoulos, Phys. Rev. D **97**, 024030 (2018).
[41] J. Ellis, G. Hütsi, K. Kannike, L. Marzola, M. Raidal, and V. Vaskonen, Phys. Rev. D **97**, 123007 (2018).
[42] A. Li, F. Huang, and R.-X. Xu, Astropart. Phys. **37**, 70 (2012).
[43] L. Tolos and J. Schaffner-Bielich, Phys. Rev. D **92**, 123002 (2015).
[44] M. Deliyergiyev, A. Del Popolo, L. Tolos, M. Le Delliou, X. Lee, and F. Burgio, Phys. Rev. D **99**, 063015 (2019).
[45] S. Mukhopadhyay, D. Atta, K. Imam, D. N. Basu, and C. Samanta, Eur. Phys. J. C **77**, 440 (2017); **77**, 553(E) (2017).
[46] J. C. Jiménez and E. S. Fraga, Universe **8**, 34 (2022).
[47] G. Panotopoulos and I. Lopes, Phys. Rev. D **98**, 083001 (2018).
[48] K.-L. Leung, M.-c. Chu, and L.-M. Lin, Phys. Rev. D **105**, 123010 (2022).
[49] O. Lourenço, T. Frederico, and M. Dutra, Phys. Rev. D **105**, 023008 (2022).
[50] T. Gleason, B. Brown, and B. Kain, Phys. Rev. D **105**, 023010 (2022).
[51] Y. Dengler, J. Schaffner-Bielich, and L. Tolos, Phys. Rev. D **105**, 043013 (2022).
[52] G. Panotopoulos and I. Lopes, Int. J. Mod. Phys. D **27**, 1850093 (2018).
[53] Z. Miao, Y. Zhu, A. Li, and F. Huang, Astrophys. J. **936**, 69 (2022).
[54] N. Rutherford, G. Raaijmakers, C. Prescod-Weinstein, and A. Watts, Phys. Rev. D **107**, 103051 (2023).
[55] B. Bertoni, A. E. Nelson, and S. Reddy, Phys. Rev. D **88**, 123505 (2013).
[56] S. A. Bhat and A. Paul, Eur. Phys. J. C **80**, 544 (2020).
[57] M. Dutra, C. H. Lenzi, and O. Lourenço, Mon. Not. R. Astron. Soc. **517**, 4265 (2022).
[58] B. Hong, Z. Ren, C. Wu, and X. Mu, Classical Quantum Gravity **40**, 125007 (2023).
[59] X. Mu, B. Hong, X. Zhou, and Z. Feng, Astrophys. Space Sci. **368**, 67 (2023).
[60] H. Zheng and L.-W. Chen, Astrophys. J. **831**, 127 (2016).
[61] E. Fonseca *et al.*, Astrophys. J. Lett. **915**, L12 (2021).
[62] M. C. Miller *et al.*, Astrophys. J. Lett. **918**, L28 (2021).

[63] T. E. Riley *et al.*, Astrophys. J. Lett. **918**, L27 (2021).
[64] B. P. Abbott *et al.* (LIGO Scientific and Virgo Collaborations), Phys. Rev. Lett. **121**, 161101 (2018).
[65] T. E. Riley *et al.*, Astrophys. J. Lett. **887**, L21 (2019).
[66] M. C. Miller *et al.*, Astrophys. J. Lett. **887**, L24 (2019).
[67] K. D. Kokkotas and B. G. Schmidt, Living Rev. Relativity **2**, 2 (1999).
[68] N. Andersson and K. D. Kokkotas, Mon. Not. R. Astron. Soc. **299**, 1059 (1998).
[69] H. K. Lau, P. T. Leung, and L. M. Lin, Astrophys. J. **714**, 1234 (2010).
[70] T. K. Chan, Y. H. Sham, P. T. Leung, and L. M. Lin, Phys. Rev. D **90**, 124023 (2014).
[71] H. Sotani and B. Kumar, Phys. Rev. D **104**, 123002 (2021).
[72] T. Zhao and J. M. Lattimer, Phys. Rev. D **106**, 123002 (2022).
[73] C. Vásquez Flores, Z. B. Hall, II, and P. Jaikumar, Phys. Rev. C **96**, 065803 (2017).
[74] B. K. Pradhan and D. Chatterjee, Phys. Rev. C **103**, 035810 (2021).
[75] A. Kunjipurayil, T. Zhao, B. Kumar, B. K. Agrawal, and M. Prakash, Phys. Rev. D **106**, 063005 (2022).
[76] K. S. Thorne and A. Campolattaro, Astrophys. J. **149**, 591 (1967).
[77] L. Lindblom and S. L. Detweiler, Astrophys. J. Suppl. Ser. **53**, 73 (1983).
[78] T. G. Cowling, Mon. Not. R. Astron. Soc. **101**, 367 (1941).
[79] H. Sotani, N. Yasutake, T. Maruyama, and T. Tatsumi, Phys. Rev. D **83**, 024014 (2011).
[80] C. V. Flores and G. Lugones, Classical Quantum Gravity **31**, 155002 (2014).
[81] N. Andersson and P. Pnigouras, Mon. Not. R. Astron. Soc. **489**, 4043 (2019).
[82] A. Kumar, P. Thakur, and M. Sinha, Mon. Not. R. Astron. Soc. **530**, 501 (2024).
[83] I. F. Ranea-Sandoval, O. M. Guilera, M. Mariani, and M. G. Orsaria, J. Cosmol. Astropart. Phys. 12 (2018) 031.
[84] C. Vásquez Flores, A. Parisi, C.-S. Chen, and G. Lugones, J. Cosmol. Astropart. Phys. 06 (2019) 051.
[85] B. K. Pradhan, D. Chatterjee, M. Lanoye, and P. Jaikumar, Phys. Rev. C **106**, 015805 (2022).
[86] O. P. Jyothilakshmi, L. J. Naik, and V. Sreekanth, Eur. Phys. J. C **84**, 427 (2024).
[87] H. C. Das, A. Kumar, S. K. Biswal, and S. K. Patra, Phys. Rev. D **104**, 123006 (2021).
[88] H.-M. Liu, J.-B. Wei, Z.-H. Li, G. F. Burgio, H. C. Das, and H. J. Schulze, Phys. Rev. D **110**, 023024 (2024).
[89] G. A. Lalazissis, J. Konig, and P. Ring, Phys. Rev. C **55**, 540 (1997).
[90] N. K. Glendenning and S. A. Moszkowski, Phys. Rev. Lett. **67**, 2414 (1991).
[91] S. Typel, G. Ropke, T. Klahn, D. Blaschke, and H. H. Wolter, Phys. Rev. C **81**, 015803 (2010).
[92] G. A. Lalazissis, T. Niksic, D. Vretenar, and P. Ring, Phys. Rev. C **71**, 024312 (2005).
[93] B.-N. Lu, E.-G. Zhao, and S.-G. Zhou, Phys. Rev. C **84**, 014328 (2011).
[94] C.-J. Xia, T. Maruyama, A. Li, B. Y. Sun, W.-H. Long, and Y.-X. Zhang, Commun. Theor. Phys. **74**, 095303 (2022).
[95] S. Tulin, H.-B. Yu, and K. M. Zurek, Phys. Rev. D **87**, 115007 (2013).
[96] D. Sen and A. Guha, Mon. Not. R. Astron. Soc. **517**, 518 (2022).
[97] S. W. Randall, M. Markevitch, D. Clowe, A. H. Gonzalez, and M. Bradac, Astrophys. J. **679**, 1173 (2008).
[98] M. Bradac, D. Clowe, A. H. Gonzalez, P. Marshall, W. Forman, C. Jones, M. Markevitch, S. Randall, T. Schrabback, and D. Zaritsky, Astrophys. J. **652**, 937 (2006).
[99] S. Tulin and H.-B. Yu, Phys. Rep. **730**, 1 (2018).
[100] T. Hambye and L. Vanderheyden, J. Cosmol. Astropart. Phys. 05 (2020) 001.
[101] G. Belanger, F. Boudjema, A. Pukhov, and A. Semenov, Comput. Phys. Commun. **185**, 960 (2014).
[102] P. Gondolo and G. Gelmini, Nucl. Phys. **B360**, 145 (1991).
[103] A. Guha, P. S. B. Dev, and P. K. Das, J. Cosmol. Astropart. Phys. 02 (2019) 032.
[104] A. Das, T. Malik, and A. C. Nayak, Phys. Rev. D **99**, 043016 (2019).
[105] A. G. Abac, C. C. Bernido, and J. P. H. Esguerra, Phys. Dark Universe **40**, 101185 (2023).
[106] R. C. Tolman, Phys. Rev. **55**, 364 (1939).
[107] J. R. Oppenheimer and G. M. Volkoff, Phys. Rev. **55**, 374 (1939).
[108] T. Hinderer, Astrophys. J. **677**, 1216 (2008).
[109] T. Hinderer, B. D. Lackey, R. N. Lang, and J. S. Read, Phys. Rev. D **81**, 123016 (2010).
[110] Z.-Y. Zheng, T.-T. Sun, H. Chen, J.-B. Wei, G. F. Burgio, and H. J. Schulze, Phys. Rev. D **107**, 103048 (2023).
[111] V. B. Thapa, M. V. Beznogov, A. R. Raduta, and P. Thakur, Phys. Rev. D **107**, 103054 (2023).